Developmental Biology 379 (2013) 76–91

Contents lists available at SciVerse ScienceDirect

Developmental Biology

journal homepage: www.elsevier.com/locate/developmentalbiology

dusky-like is required to maintain the integrity and planar cell polarity of hairs during the development of the Drosophila wing

Paul N. Adler [a,b,*], Lukasz F. Sobala [a], DeSean Thom [a], Ranganayaki Nagaraj [a]

[a] Biology Department, Institute for Morphogenesis and Regenerative Medicine, University of Virginia, Charlottesville, VA 22903, USA
[b] Cell Biology Department, Institute for Morphogenesis and Regenerative Medicine, University of Virginia, Charlottesville, VA 22903, USA

ARTICLE INFO

Article history:
Received 12 October 2012
Received in revised form
11 February 2013
Accepted 4 April 2013
Available online 23 April 2013

Keywords:
dyl
Drosophila
Wing hair
Chitin
Planar polarity

ABSTRACT

The cuticular hairs and sensory bristles that decorate the adult Drosophila epidermis and the denticles found on the embryo have been used in studies on planar cell polarity and as models for the cytoskeletal mediated morphogenesis of cellular extensions. ZP domain proteins have recently been found to be important for the morphogenesis of both denticles and bristles. Here we show that the ZP domain protein Dusky-like is a key player in hair morphogenesis. As is the case in bristles, in hairs *dyl* mutants display a dramatic phenotype that is the consequence of a failure to maintain the integrity of the extension after outgrowth. Hairs lacking *dyl* function are split, thinned, multipled and often very short. *dyl* is required for normal chitin deposition in hairs, but chitin is not required for the normal accumulation of Dyl, hence *dyl* acts upstream of chitin. A lack of chitin however, does not mimic the *dyl* hair phenotype, thus Dyl must have other targets in hair morphogenesis. One of these appears to be the actin cytoskeleton. Interestingly, *dyl* mutants also display a unique planar cell polarity phenotype that is distinct from that seen with mutations in the *frizzled/starry night* or *dachsous/fat* pathway genes. Rab11 was previously found to be essential for Dyl plasma membrane localization in bristles. Here we found that the expression of a dominant negative Rab11 can mimic the *dyl* hair morphology phenotype consistent with Rab11 also being required for Dyl function in hairs. We carried out a small directed screen to identify genes that might function with *dyl* and identified *Chitinase 6* (*Cht6*) as a strong candidate, as knocking down *Cht6* function led to weak versions of all of the *dyl* hair phenotypes.

Introduction

The adult cuticle of Drosophila is decorated with a variety of polarized extensions. These include bristle sense organs and non-sensory hairs (trichomes) and arista laterals (Adler, 2002; He and Adler, 2001; Tilney et al., 2000; Wong and Adler, 1993). The larger of these structures (bristle shafts and arista laterals) are formed by polyploid cells while epidermal hairs are produced by outgrowths from the apical surface of diploid cells. All of these extensions involve both the actin and microtubule cytoskeletons (Geng et al., 2000; Tilney et al., 2000; Turner and Adler, 1998) and many genes have been found to be important in the morphogenesis of all 3 cell types. However, mutations in some genes do not produce equivalent phenotypes in these cell types or in the related denticles that decorate larvae (Fernandes et al., 2010; Price et al., 2006). This could be due to the great difference in size or in other extension specific properties.

The array of distally pointing hairs on the wing of Drosophila has been used extensively in studies on planar cell polarity (PCP) (Adler, 2002, 2012; Amonlirdviman et al., 2005; Goodrich and Strutt, 2011; Lawrence et al., 2007; Strutt, 2002; Wu and Mlodzik, 2009). As an aid to such studies some years ago we characterized changes in pupal wing gene expression around the time of hair morphogenesis (Ren et al., 2005). More than 1300 genes were identified where a greater than twofold change in expression was seen and 436 where a fivefold or greater change was detected. One of the genes that stood out was CG15013, which is also known as *dusky-like* (*dyl*). Dyl contains a ZP (zona pellucida) domain, which has been found in a number of transmembrane and secreted proteins that are thought to organize the apical extracellular domain and perhaps in some contexts link it to the actin cytoskeleton (Fernandes et al., 2010; Plaza et al., 2010). The expression of *dyl* increased 118fold from the start to late in the process of hair mophogenesis. Recently *dyl* and other genes that encode ZP domain proteins were shown to play a key role in the morphogenesis of first larval instar denticles and different ZP proteins were found to localize to different parts of the denticle (Fernandes et al., 2010). Differences in mutant phenotypes reflected the differences in protein localization and suggested that at least some ZP domain proteins link cuticle to the apical plasma membrane. Further, we recently found that *dyl* function was required for the formation of normal cuticle in adult sensory bristles (Nagaraj and Adler, 2012). We additionally established that Dyl functioned as a Rab11 effector for chitin deposition and that Rab11 function was required for the localization of Dyl in the plasma membrane.

* Corresponding author at: Biology Department, Institute for Morphogenesis and Regenerative Medicine, University of Virginia, Charlottesville, VA 22903, USA. Fax: +1 434 983 5626.
E-mail address: pna@virginia.edu (P.N. Adler).

0012-1606/$ - see front matter © 2013 Elsevier Inc. All rights reserved.
http://dx.doi.org/10.1016/j.ydbio.2013.04.012

Here we report that *dyl* is also important for wing hair morphogenesis. *dyl* loss of function leads to thin, split and multipled hairs and the Dyl protein accumulated in hairs. Interestingly, the mutant phenotype was not due to an effect on hair growth. Rather, the abnormalities were first detected after hair outgrowth was largely complete. This was very similar to the phenotype seen in sensory bristles where the adult stub bristle phenotype was associated with bristle collapse and not a failure in growth (Nagaraj and Adler, 2012). We also saw abnormalities in chitin deposition in these wings consistent with the role for *dyl* in cuticle formation seen previously in both embryonic denticles and in sensory bristles (Fernandes et al., 2010; Nagaraj and Adler, 2012). In contrast chitin was not required for the normal accumulation of Dyl in growing hairs, thus Dyl acts upstream of chitin. In addition to the hair morphology abnormalities seen with a reduction in Dyl we also found that the normal parallel alignment of neighboring hairs was degraded. This late planar cell polarity phenotype was somewhat reminiscent of phenotypes seen in mutations in genes that encode septate junction components (Moyer and Jacobs, 2008; Venema et al., 2004), but unique in detail. We also found that the directed and premature expression of *dyl* led to multiple and branched wing hairs. This was seen in both growing pupal wings and in adult wings and appeared to be due to effects on the cytoskeleton and not on chitin/cuticle deposition.

Evidence for a role for Rab11 in hair morphogenesis was recently provided by several groups (Gault et al., 2012; Purvanov et al., 2010), although no evidence for a *dyl* like phenotype was reported. We found the directed expression of dominant negative Rab11 was able to produce phenotypes that mimicked the *dyl* hair phenotypes. We also observed that Rab11 is found in growing hairs and accumulated at the distal tip of the hair. This localization pattern is similar to what is seen in sensory bristles (Nagaraj and Adler, 2012). An interesting finding in our experiments was a *frizzled/starry night* (*fz/stan*) like PCP phenotype (Adler, 2002, 2012; Goodrich and Strutt, 2011; Lawrence et al., 2007; Wu and Mlodzik, 2009) in wings where the DN-Rab11 was expressed and that this was associated with a disruption of the normal asymmetric accumulation of the Stan and Inturned proteins. This may be due to effects on the intracellular transport needed to form the proximal and distal PCP protein complexes.

The *dyl* hair kd phenotype shared some characteristics with that seen for mutations in *kkv*, which encodes chitin synthase (Devine et al., 2005; Moussian et al., 2005; Ostrowski et al., 2002; Ren et al., 2005). However, *kkv* mutations did not result in the branching and multiple hairs produced by *dyl* mutants hence a lack of chitin deposition cannot explain the *dyl* mutant phenotype. The expression of *kkv* also changes dramatically during hair morphogenesis (Ren et al., 2005). In an attempt to identify additional genes that might function along with *dyl* and *kkv* we screened 103 genes whose expression is strongly modulated during the terminal differentiation of Drosophila epidermal cells (Ren et al., 2005). A knock down of 45 lead to a phenotype that was at least somewhat reminiscent of that seen in *dyl* or *kkv* mutants. Some of these are likely play a role in cuticle formation. The most notable was *Chitinase 6* (*Cht6*), whose expression also dramatically increases late in hair morphogenesis (Ren et al., 2005). Reducing *Cht*6 activity in wing cells resulted in a weak version of all of the phenotypes seen with *dyl*.

Materials and methods

Fly culture and strains

All flies were grown on standard media. Oregon R was used as a wild type control. The *kkv*, *Rab11* and *dyl* mutant and deficiency lines were obtained from the Bloomington *Drosophila* stock center at Indiana University unless stated otherwise. Most of the stocks used for generating *flp*/FRT somatic clones and the *Gal4* driver lines were also obtained from the Bloomington stock center. The *UAS-Rab11dsRNA pWIZ* stock was provided by D. Ready; $rab11^{93Bi}$/TM6, $rab11^{ex1}$/TM6, $Rab11^{\Delta FRT}$/*TM6*, and *y w hs-flp; FRT5377 hrp-GFP/TM3* by R. Cohen; The UAS-*dyl* stocks and the anti-Dyl antibodies were kindly provided by F. Payre. Stocks used to induce RNAi were obtained from the Vienna Stock Center (V lines) and from the stock center in Bloomington (T lines from the Harvard collection). Key lines for RNAi experiments included V102166 (*dyl*) and V107916 (Cht6). The line that carried a UAS dominant negative Rab11 transgene was obtained from the Bloomington stock center (B-23261). An alternative stock that carried a similar transgene did not express well (B-9790) in our hands.

A screen to identify additional genes that shared aspects of the *dyl* and/or *kkv* mutant phenotypes was done by crossing *UAS-geneX-dsRNA* females to *UAS-dicer2; ptc-Gal4* males. This resulted in females where RNAi was enhanced by the *dicer-2* expressing transgene and males where this was not the case. This allowed us in one cross to be able to see the enhanced phenotype and if this was lethal the unenhanced one. The larvae and pupae were cultured at 25 °C. In cases where even the unenhanced males died under these conditions vials were moved to 21 °C or 18 °C, which results in lower Gal4 activity and hence a weaker RNAi effect. In several cases this resulted in viability that allowed us to score for a possible wing phenotype.

Generation of kkv, rab1, and dyl kd and oe clones

Clones where *dyl* was knocked down were generated by crossing *w hs-flp*; *AyGal4 UAS-lacZ*; *UAS-dicer 2* females and *UAS-dyl-RNAi* males. Vials were heat shocked for 20 min to induce clones. A similar protocol was used to generate clones that over-expressed (oe) *dyl* by substituting males that carried *UAS-dyl* instead of *UAS-dyl-RNAi. kkv* mutant clones were generated by crossing *w hs-flp*; *FRT82 Ubi-GFP/TM6* females to FRT82 kkv^1 e/TM6 males (Xu and Rubin, 1993). Vials were heat shocked at 37 °C for 1 h to induce *flp* and clone formation. $Rab11^{ex1}$ clones were induced in an analogous experiment. $Rab11^{\Delta FRT}$ clones were induced as described by Bogard et al., (2007). To examine the consequences of a reduction in *dyl* function in cells that lacked *kkv* we generated flies that were *w hs-flp*; *ptc-Gal4/UAS-dyl-RNAi*; *FRT82* kkv^1 *e/FRT82 flies*. These flies were heat shocked to induce *kkv* clones and we compared the phenotypes of the clones inside and outside of the *ptc* domain where *dyl* was kd. Flies carrying *kkv* clones often died prior to or soon after eclosion. Others were unable to “pump out” their wings. These problems appear to be due to a failure in the cuticular barrier that separates the cells and hemolymph from the external world (Nagaraj and Adler, 2012). To minimize this we tried to limit clones to a very small size by delaying heat shocking until at least the wandering third instar stage. Perdurance is not a problem for *kkv* clones due to the dramatic increase in expression of the gene in wing cells during the second day of pupal life (Ren et al., 2005).

Immunostaining

Immunostaining was done by standard protocols (e.g. see (He et al., 2005) on paraformaldehyde fixed material. Primary antibodies were used at the following concentrations: Rabbit anti-GFP (1:4000 Molecular Probes), mouse anti-GFP (1:1000 Molecular Probes), mouse anti-B-galactosidase (Developmental Studies Hybridoma Lab (1:1000)(Mab 40-1) and anti-Dyl (1:1–2000)) (kindly provided by F. Payre; or 1:5000 our independently isolated antibody, which is directed against a segment in the extra-cellular domain). Alexa 488 and Alexa 568 conjugated secondary antibodies (1:250) were purchased from

Molecular Probes. For F-actin staining we used Alexa Flour Phalloidin (488, 568 or 647) (Molecular Probes).

Chitin staining using CBD-Rhodamine probe

To visualize chitin, pupal wings were fixed and incubated in a 1:200 dilution of the Rhodamine conjugated chitin binding probe (New England Biolabs) (Gangishetti et al., 2009) in phosphate-buffered saline (PBS) containing 0.3% Triton X-100 for 2–4 h at room temperature, rinsed in PBS and mounted. This staining procedure was combined serially with other staining protocols in a number of experiments (Nagaraj and Adler, 2012). The chitin staining (always done first) often lead to less than optimal results for the other staining (e.g. phalloidin or antibody), but adequate results were usually possible.

Image analysis

Confocal images were obtained using a Zeiss Meta laser scanning confocal scope at the Keck Center for Cellular Imaging at the University of Virginia or a CARV spinning disc unit on a Nikon Eclipse TE200 microscope controlled by Metamorph software. Cuticle images were obtained using a Spot digital camera (National Diagnostics) on a Zeiss Axioskop 2 microscope. Images were analyzed using Image J and processed using Adobe Photoshop.

Analysis of hair polarity

We first attempted to quantify the PCP phenotype of *dyl* by examining hair polarity using an automated approach with the Metamorph or ImageJ software. Both of these programs did a good job in recognizing and measuring the polarity of wild type hairs but they had difficulties with the thinner, branched and occasionally crossed *dyl* hairs. Hence we manually measured hair orientation for both wild type and *dyl* mutant hairs using ImageJ. We did not score mutant hairs that were branched or otherwise highly abnormal in structure. The data presented is all from the middle of the D cell of the wing (distal to the posterior cross vein) however Qualitatively similar results were obtained from the other two regions we examined in preliminary experiments. Qualitatively similar results were also obtained from examining wings both by light microscopy (when mounted) and SEM. The data was analyzed using the Oriana software package (Kovach Computing Services).

Results

dyl functions cell autonomously in hair morphogenesis

To examine the role of *dyl* in hair morphogenesis we used transgene mediated RNAi to knock down (kd) *dyl* function. When *ptc*-Gal4 was used to kd expression in a stripe down the middle of the wing we observed the hairs were more upright than normal and often much thinner. Many of the hairs were multipled and/or split and there were stubs that likely represented collapsed hairs (Fig. 1A–C, F). Some hairs also appeared curved. These were somewhat difficult to image in the light microscope and more detail could be seen using scanning electron microscopy (Fig. 1A–C). In the SEM we could also see prominent “cups” surrounding the hairs (Fig. 1B, C arrowheads). Less prominent “cups” could often be seen in wild type wings. These may represent a remnant of the hair pedestals identified many years ago by Mitchell, Petersen and colleagues (Mitchell et al., 1990). We refer to this collection of hair morphology phenotypes as the “*dyl* hair phenotype”.

In experiments on both embryonic denticles and on adult bristles the *dyl* kd phenotype was found to be specific to the *dyl* gene (Fernandes et al., 2010; Nagaraj and Adler, 2012). To confirm that the kd phenotype was also specific for the wing hair phenotype we examined wings of adult escapers that were either homo or hemizygous for a hypomorphic allele of *dyl* ($dyl^{MI02088}$). The wings of these flies showed a weak version of the kd phenotypes with somewhat thinned and occasionally split hairs and hair cups confirming the specificity of the kd phenotype (Fig. 1G, H arrows and arrowheads respectively).

The phenotype of the *ptc-Gal4* driven kd wings indicated that *dyl* did not act systemically. However, because *ptc* expression levels decrease in a gradient as one moves laterally away from the midline those observations did not rule out short distance non-autonomy for *dyl*. To examine the cell autonomy of the *dyl* kd we induced flip out clones (Struhl and Basler, 1993). In adult wings examined by either SEM or light microscopy the clones could be identified by groups of cells that had the *dyl* hair phenotype that were directly juxtaposed to normal hairs (Fig. 2A, B). These observations suggested that the kd acted cell autonomously. To test this more rigorously we examined pupal wing clones marked by the expression of LacZ (Fig. 2F–I). In these experiments the *dyl* mutant phenotype was only seen in the marked cells and there was no evidence of rescue by neighboring wild type cells. We concluded that the *dyl* hair phenotype is cell autonomous.

dyl is essential for the maintenance of hair integrity

To determine if the *dyl* hair phenotype was due to a direct effect on hair growth we examined pupal wings where *dyl* was kd in the *ptc* domain (Fig. 3A–C). We observed that hair outgrowth began precociously in the kd cells (Fig. 3A) and that for several hours those hairs appeared morphologically normal although more advanced/substantial than neighboring control hairs (Fig. 2F, G; Fig. 3B). Around 38–41 h awp, when hair growth is largely complete the *dyl* kd hairs became thinned, bent, split, collapsed and multipled and began to take on the morphology of the adult kd hairs (Fig. 3C, D). We similarly examined *dyl* kd flip out clones and also found the morphological abnormalities were not seen in growing hairs—only in older hairs (Fig. 2F–I). Thus, the adult *dyl* hair phenotype is not due to a defect in growth, rather one in the maintenance of hair morphology.

Since the *dyl* bristle phenotype is associated with altered chitin deposition (Nagaraj and Adler, 2012) we examined chitin deposition in both wild type and *dyl* kd wings. In wild type wings hair outgrowth starts around 32 h awp and by about 40 h awp it is largely complete (Mitchell et al., 1990; Wong and Adler, 1993). Around this time wing expansion begins (Mitchell et al., 1990). This process leads to a flattening of the cuboidal pupal wing cells and a large increase in the apical surface of the wing (Fig. S1). The first sign of this is a slight curving in the proximal posterior region of the wing. As the wing expands and lengthens along the proximal distal axis two folds appear on the distal posterior region of the wing. The continued expansion leads to the wing folding back so that the distal tip is pointed proximally. At the early stages of this process we observed a dramatic accumulation of F-actin foci just under the apical plasma membrane (in the apical 1 μm of the wing cells) (Fig. S1). Once expansion had proceeded to the extent that the start of folding was seen we were able to detect chitin by staining with a fluorescent chitin binding protein (Fig. S1). We suggest that the increase in F-actin foci is associated with exocytosis and the deposition of cuticle. This did not appear to be dramatically altered in the *dyl* kd. A few hrs later when in wild type a small disc of F-actin is seen at the base of wild type hairs (Fig. 3E) (Roch et al., 2003) the *dyl* kd hairs showed a dramatically enhanced F-actin disc (Fig. 3H).

The enhanced actin staining was seen at all stages where basal discs were present. We suggest this is the cause of the cup-like structure seen in the SEM of kd wings. We found that chitin staining was present but abnormal in the *dyl* kd hairs (Fig. 3G, J). In wild type hairs at this time the hair is long and gently tapered. The hair still stains strongly for F-actin and chitin staining is seen smoothly and relatively evenly outlining the F-actin staining all along the hair. In the mutant hairs both F-actin and chitin staining were abnormal. Hair F-actin staining was reduced distally and chitin staining was both reduced distally and much stronger proximally.

Dyl and PCP

In adult wings where *dyl* expression was knocked down during hair morphogenesis we noted that the orientation of hairs was abnormal with many hairs pointing 30° or more from distal (Fig. 1A). Hairs often stood more erect than normal and neighboring hairs were not well aligned. This was not due to a disturbance of hair polarity during mounting as the abnormal polarity was restricted to the *ptc* domain and the SEM samples were not mounted between a cover slip and a microscope slide. Further,

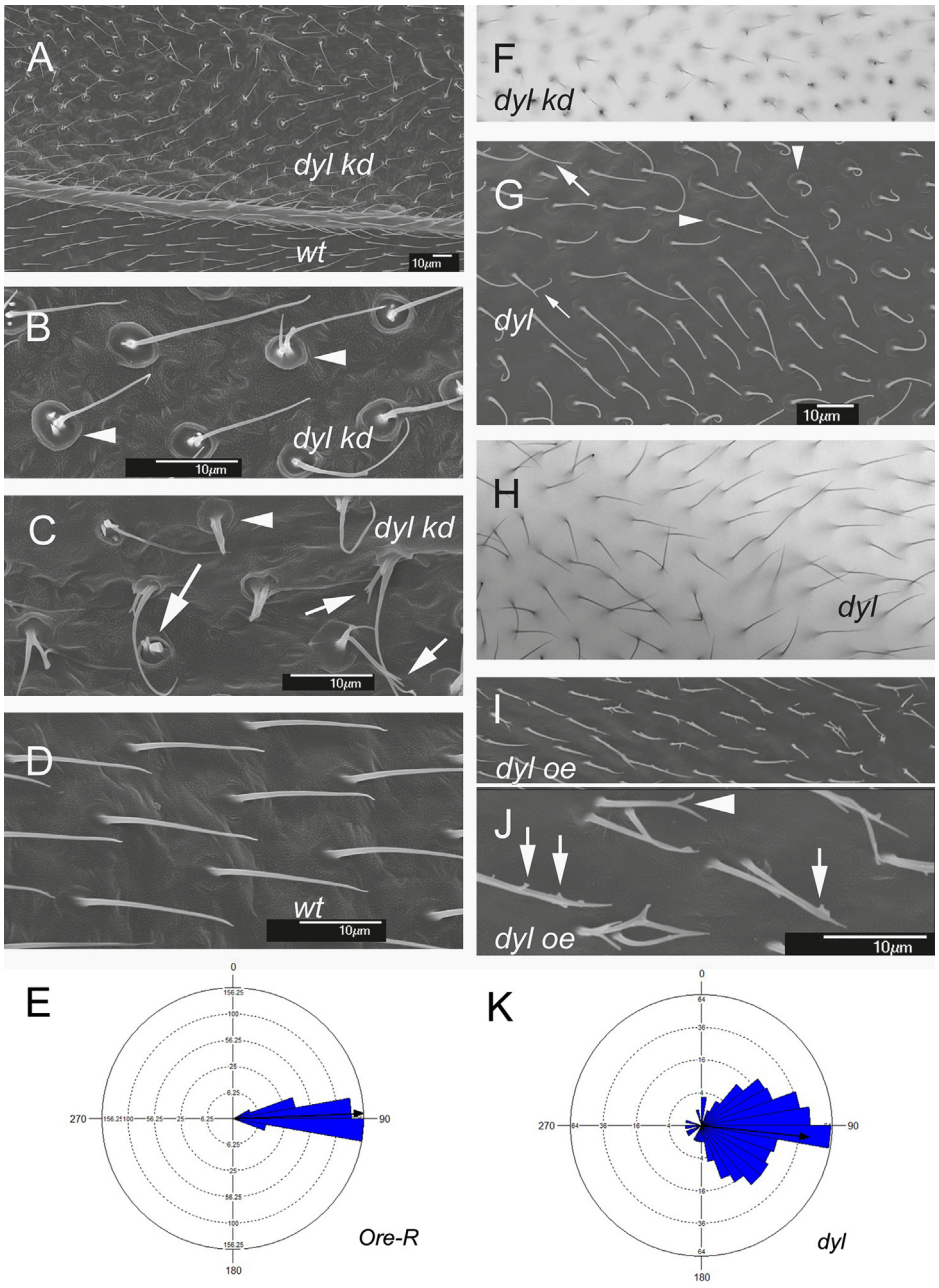

Fig. 1. Dyl functions in hair morphogenesis. (A) An SEM of an adult *ptc-Gal4 UAS-dyl RNAi* wing. The *ptc* domain includes the region above the vein shown in the image (marked by *dyl* kd). Note the hair polarity phenotype. (B) A high mag SEM of an adult *ptc-Gal4 UAS-dyl* wing. The arrowheads point to the hair "cups". (C) A high mag SEM of an adult *ptc-Gal4 UAS-dyl* wing. The arrowhead points to a hair "cups". The arrows point to thin and/or branched *dyl* kd hairs. (D) An SEM of phenotypically wild type hairs from outside of the *ptc* domain of the *ptc-Gal4 UAS-dyl RNAi* wing in (A). (E) A Rose diagram showing the distribution of hair orientation for Ore-R wings. The arrow shows the mean orientation. (F) A bright field micrograph of the phenotype associated with a *dyl kd* (*ptc-Gal4 UAS-dyl RNAi*). (G) An SEM of a $dyl^{MI02088}/Df$ wing. Note the abnormal hair polarity. The larger arrow points to a thin hair, the smaller arrow to a split hair and the arrowheads to "cups" at the base of *dyl* mutant hairs. (H) A bright field micrograph of a $dyl^{MI02088}/Df$ wing. Note the poor alignment of neighboring hairs. (I) An SEM of a *ptc-Gal4 UAS-dyl* wing. (J) A higher mag SEM of a *ptc-Gal4 UAS-dyl* wing where the small branches (arrows) and split (arrowheads) can be seen. (K) A Rose diagram showing the distribution of hair orientation for $dyl^{MI02088}/Df$ wings. The arrow shows the mean orientation. Note how much broader the distribution is than in *Ore-R*.

the polarity disruption was also observed in the light microscope in wings simply placed on a slide without mounting media or a cover slip (Fig. S2A). We also observed mutant hairs with abnormal polarity next to wild types hairs of normal polarity in flip out kd clones observed without mounting (Fig. S2B, C). Hence, mounting is unrelated to the polarity phenotype. Since the kd hairs showed normal polarity at early and mid-stages of growth in the pupal wing the kd is not altering the subcellular site for hair initiation as do mutations in the *fz/stan* pathway (Wong and Adler, 1993) and *ds/ft* pathway genes (Adler et al., 1998). The disruption of local alignment phenotype was quite prominent in parts of the wings of $dyl^{MI02088}/Df$ flies (Fig. 1G, H). We took advantage of these wings to quantify the abnormal hair polarity as described in the methods. As expected from simple observation wild type wings showed a tight distribution of hair orientations (Fig. 1E), while the distribution was markedly broader in the mutant (Fig. 1K). For example, less than 1% (3/331) *Ore-R* hairs were oriented more than 20° from distal, while almost 50% (164/330) of $dyl^{MI02088}/Df$ hairs were. The two populations of hairs were significantly different in terms of orientations ($p < 10^{-12}$ Marida–Watson–Wheeler; $p < 0.001$ Watson U^2).

The poor alignment of neighboring hairs and the lack of an effect on the site of prehair initiation is reminiscent of the phenotype seen with mutations in genes that encode components of the septate junction such as Gliotectin (Moyer and Jacobs, 2008; Venema et al., 2004). As was described previously this abnormal polarity is associated with the hair pedestal/base not being parallel to the blade surface (Fig. S3). Thus, this polarity phenotype is not a mimic of the *dyl* phenotype, which represents a novel planar cell polarity phenotype.

Dyl accumulates in growing hairs

Based on what is known about ZP domain proteins it seemed likely that Dyl functioned in the hair to mediate chitin deposition and to insure the maintenance of hair structure (Fernandes et al., 2010; Nagaraj and Adler, 2012; Plaza et al., 2010). We immunolocalized Dyl in developing pupal hairs and found that Dyl accumulated in extending hairs (Fig. 4) consistent with it acting locally as expected. Dyl levels remained high throughout hair outgrowth and the period of chitin deposition and at late stages appeared

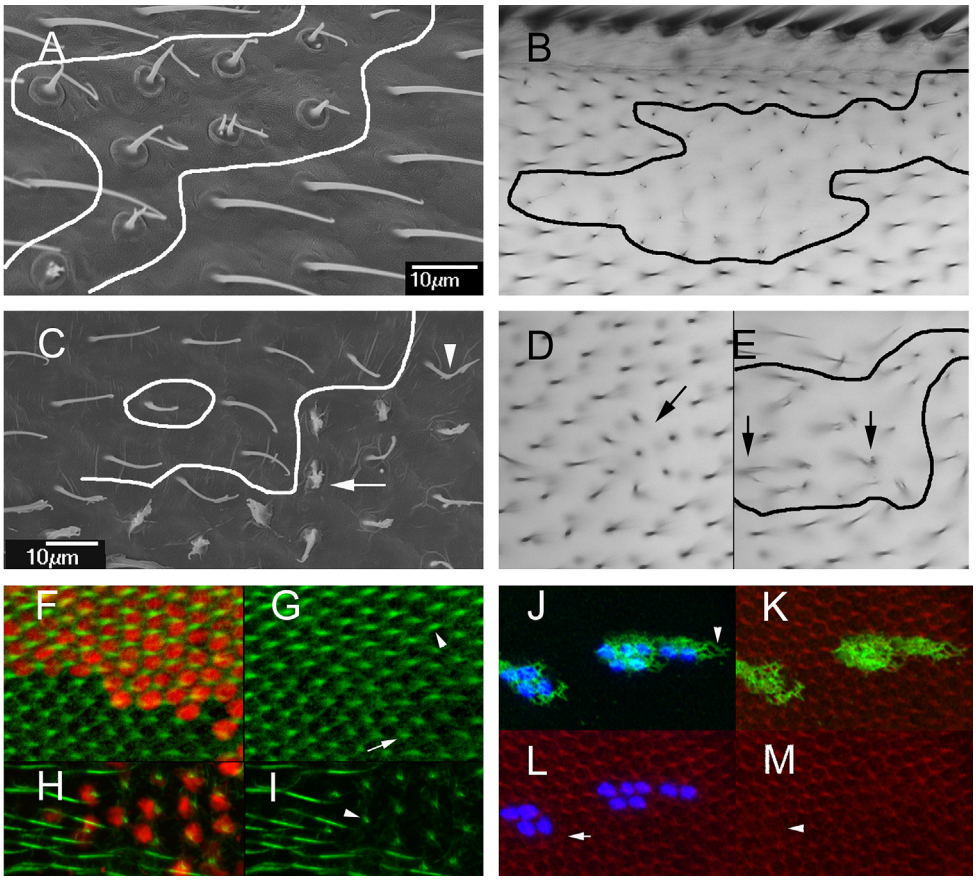

Fig. 2. Cell autonomy of *dyl*. (A) An SEM of a *dyl* kd flip out clone. The putative clone boundary is outlined. Note the strong *dyl* phenotype of the putative clone cells juxtaposed to wild type hairs. (B) A light micrograph showing of a *dyl* kd flip out clone. Once again note the wild type cells that are juxtaposed next to cells that show a strong *dyl* mutant phenotype. (C) An SEM of a *dyl oe* flip out clone. Note some cells show a very strong phenotype (arrow), some a weak phenotype (arrowhead) and others appear wild type. (D) A bright field micrograph of a small *dyl* oe clone. A small group of hairs appear to point inward (arrow). (E) A bright field micrograph of a larger *dyl* oe clone. The putative clone is outlined. As was observed in the SEM such clones contain cells that display a range of phenotypes. The arrows point to abnormal hairs. (F) A *dyl* kd flip out clone in a 33 h pupal wing marked by the expression of LacZ (red). F-actin (green) shows the growing hairs. (G) The same wing as in F but with only the green (F-actin) channel. Note the clone hairs (arrowhead) are of wild type morphology at this stage and appear longer on average than the wild type neighbors (arrow). (H) A *dyl* kd flip out clone in a 46 h pupal wing marked by the expression of LacZ (red). F-actin (green) shows the growing hairs. (I) The same wing as in H but with only the green channel shown. The phenotype of the *dyl* hairs is dramatic while neighboring wild type hairs show no phenotype. At this late stage F-actin staining is less vigorous and consistent from hair to hair than in younger wings particularly when combined with antibody staining. (J) A flip out *dyl* oe clone marked by the expression of LacZ (blue). Note the accumulation of Dyl is fibrous and extends beyond the clone cells (arrowhead). Note that the endogenous Dyl found in hairs is not visible at this level of exposure. (K) The same cells as in J with F-actin staining shown. (L) The same cells as in J with actin and LacZ shown. Note that some wild type cells show abnormal hair F-actin (arrow). (M) The same cells showing only F-actin staining. Note that some kd cells also display abnormal hair F-actin (arrowhead).

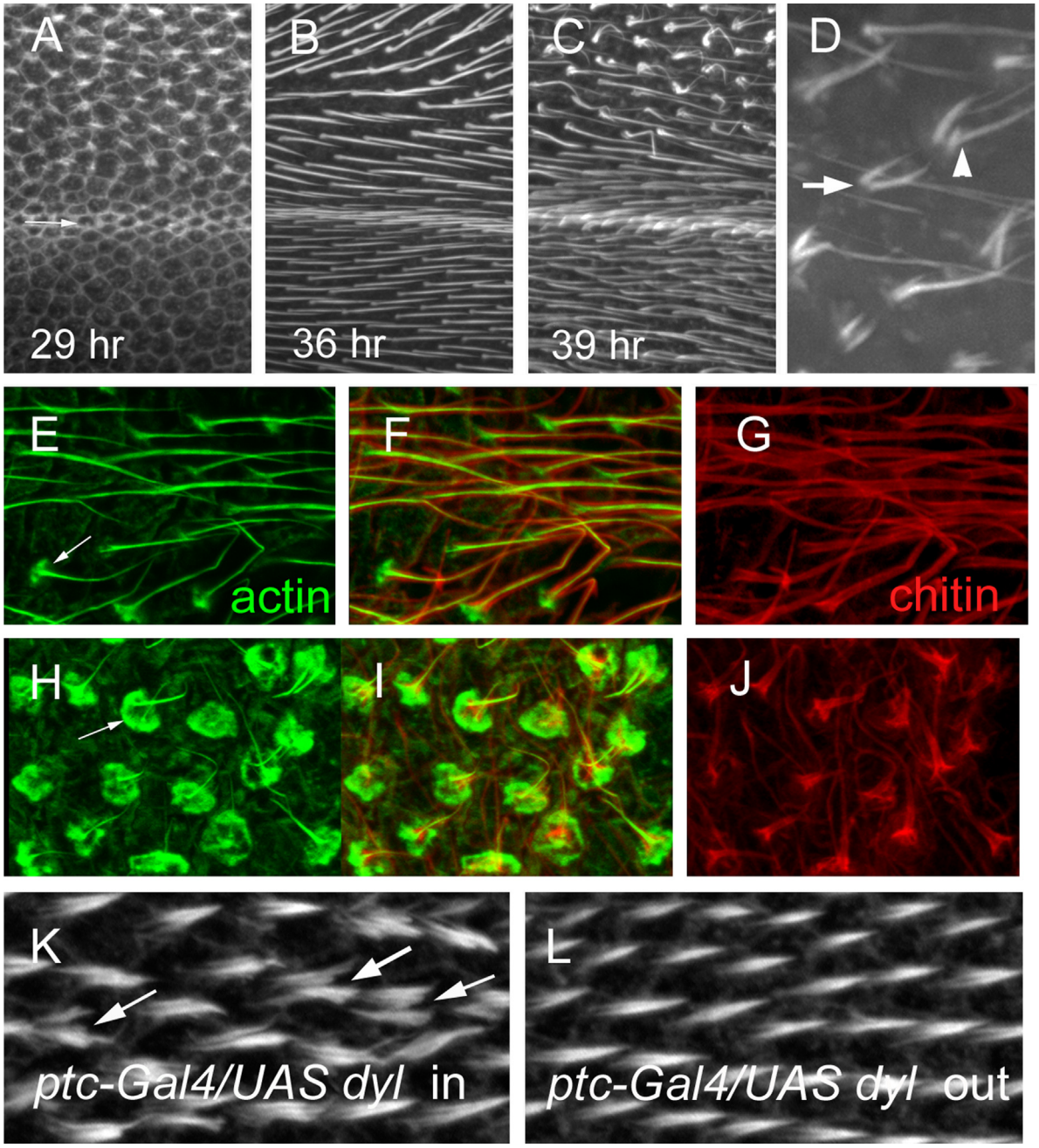

Fig. 3. Dyl and hair morphogenesis. (A) A 29 h *ptc-Gal4 UAS-dyl RNAi* pupal wing stained to show F-actin. The arrow shows the boundary between the *ptc* domain and the wild type wing posterior to it (below). Note the hairs forming inside the *ptc* domain and not outside it. (B) A 36 h *ptc-Gal4 UAS-dyl RNAi* pupal wing stained for F-actin. Hairs are seen both in and outside of the *ptc* domain, but note the hairs inside the *ptc* domain appear longer, thicker and are stained more brightly. (C) A 39 h *ptc-Gal4 UAS-dyl RNAi* pupal wing stained for F-actin. Note hairs inside the *ptc* domain are starting to appear abnormal. (D) A higher magnification view of abnormal *ptc-Gal4 UAS-dyl RNAi* hairs in a 39 h wing. The arrow points to a multiple hair cell. The arrowhead points to a split hair. (E) A 43 h *ptc-Gal4 UAS-dyl RNAi* pupal wing stained for F-actin. This image is from a region outside of the *ptc* domain. Note the F-actin (green) in the hair is central to chitin (red). Relatively weak staining of hair cups is visible (arrow). (F) A merged image of E and G. (G) The same wing region shown in E, but stained for chitin in red. (H) A 43 h *ptc-Gal4 UAS-dyl RNAi* pupal wing stained for F-actin. This image is for a region inside of the *ptc* domain. The arrow points to the large accumulation of F-actin at the base of the hair and the abnormal structure of the hairs. (I) A merge of H and J. (J) The same wing region shown in H, but stained for chitin in red. Note the staining is far brighter in the proximal part of the hair. This is not seen in wt. (K) A 33 h *ptc-Gal4 Tub-Gal80^{ts} UAS-dyl* pupal wing inside of the *ptc* domain. The arrow points to a multiple/split hair cell. (L) A 33 h *ptc-Gal4 Tub-Gal80^{ts} UAS-dyl* pupal wing outside of the *ptc* domain. Note that the relative total hair F-actin staining is on average slightly stronger in K than L.

more prominent at the base of the hair (Fig. S4). We did not see substantial Dyl immunostaining prior to hair initiation consistent with the dramatic increase in Dyl mRNA levels from 32 h to 40 h awp. Based on the precocious hair initiation kd phenotype Dyl is expected to be present earlier than 32 h awp. Our failure to detect it is likely due to our antibody reagent not being sensitive enough. It is also possible that Dyl is not localized to a particular subcellular region prior to hair outgrowth making its detection more difficult. As a control for the specificity of the antibodies we immunostained pupal wings where *dyl* was kd in the *ptc* domain. There was a dramatic loss of immunostaining in this region confirming the specificity of the antibody reagent for immunostaining pupal wings (Fig. S4).

A dyl gain of function hair morphology phenotype

We carried out complementary experiments where we over expressed (oe) *dyl* using *ptc-Gal4*. In such experiments *dyl* is also

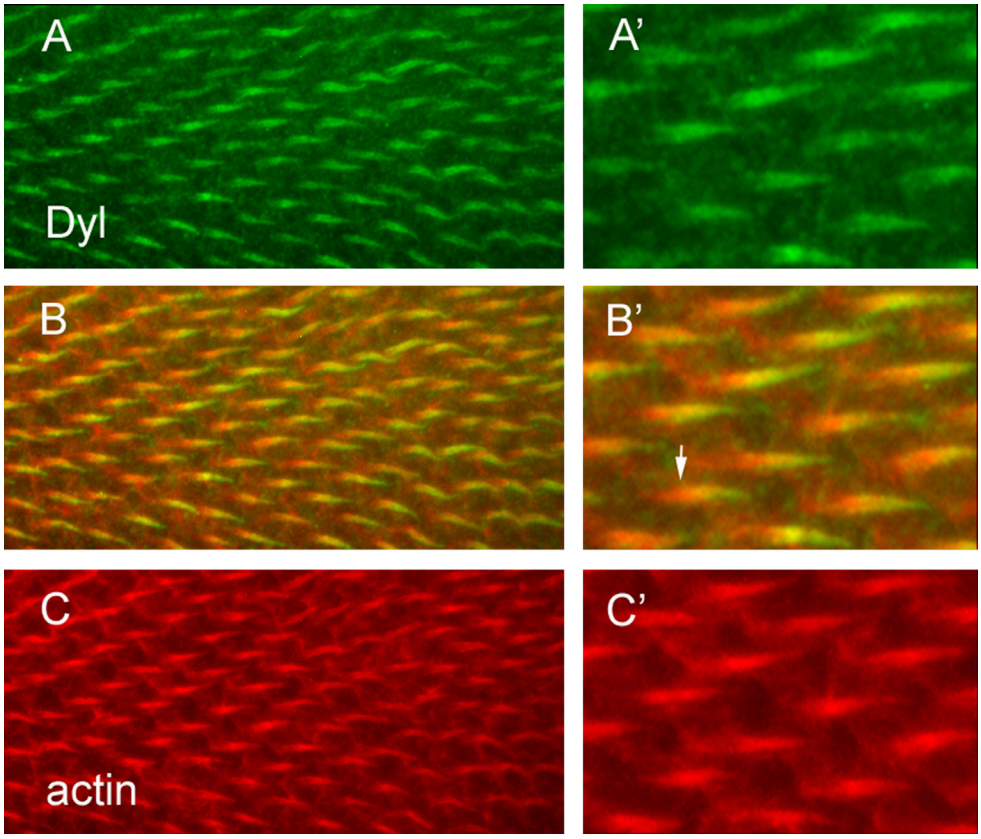

Fig. 4. Dyl accumulates in growing hairs. (A) Dyl antibody staining shows the protein accumulates in growing hairs. (B) A merge of A and C. (C) F-actin staining. (A′) A higher magnification image of part of the field in A. (B′) A higher magnification image of part of the field in B. The arrow points to the proximal "root" of the hair that stains for actin but not the plasma membrane localized Dyl. (C′) A higher magnification image of part of the field in C.

expressed throughout development as opposed to being strongly modulated as a function of time in wing cells. For simplicity we will use oe in discussing such experiments. We found extensive lethality among *ptc > dyl* animals and needed to restrict the time of expression by co-expressing a temperature sensitive Gal80 protein and utilizing a temperature shift. Under these conditions we found that the over expression of *dyl* during the time between wpp formation and hair outgrowth resulted in multipled and branched hairs. These were not thinned as we observed in the *dyl* kd hairs. The pattern of branching was quite dramatic in some cases. Due to the small size of many of the branches they were best seen by the use of scanning electron microscopy (Fig. 1I, J). We also examined in pupal wings the consequences of *dyl* over expression (Fig. 3K L). We observed multiple and split hairs at all stages of growth (Fig. 3K, L), hence this phenotype is not due to an effect on hair maintenance or cuticle deposition, which begins about 10 h after hair initiation. Rather the multiple/split hair cell phenotype is likely due to effects on the cytoskeleton. The *dyl* oe pupal hairs often appeared thicker than their wild type neighbors particularly if one adds together the multiple and split hairs. Hence there appears to be more "hair volume" and more total hair F-actin associated with *dyl* oe. In some of these experiments we noticed what appeared to be a slight delay in hair initiation. This gain of function phenotype interfered with transgene rescue experiments.

We also examined flip out clones where *dyl* was over expressed. Surprisingly, the phenotypes of cells in the center of the clones appeared to be generally more severe than hairs at the periphery (Fig. 2C–E). Since there was no cell marker in this experiment we could not determine if the clone cells were influencing their wild type neighbors or if the wild type cells were partly rescuing juxtaposed oe cells. We examined flip out clones in pupal wings and observed by immunostaining that the oe Dyl extended beyond the clone, which was marked by the expression of LacZ (Fig. 2J arrow, Fig. S5A, B). In most cases this effect was modest but in some clones the oe Dyl extended many cells beyond the clone (Fig. S5A, B). Interestingly, there appeared to be a bias for the oe Dyl to be found distal to the clone. The oe Dyl was apical to the cell (Fig. S5), appeared to be in a fibrous

Fig. 5. Rab11 and wing development. (A) A *ptcGal4 Gal80^{ts}/UAS-DN-Rab11* wing from a fly grown at 21 °C. (B) A *ptcGal4 Gal80^{ts}/UAS-DN-Rab11* wing from a fly grown at 27.5 °C. The arrow points to the reduced size of the *ptc* domain. (C) A micrograph of a *ptcGal4 Gal80^{ts}/UAS-DN-Rab11* wing from a fly grown at 27.5 °C. Just distal to the anterior cross vein (ACV) is a group of cells showing abnormal hair polarity (arrows) and multiple hair cells (arrowheads). (D) A micrograph of a *ptcGal4 Gal80^{ts}/UAS-DN-Rab11* wing from a fly grown at 21 °C until wpp and then shifted to 27.5 °C. Note the presence of several thin split hairs (arrows). (E) A micrograph of a *ptcGal4 Gal80^{ts}/UAS-DN-Rab11* wing from a fly grown at 21 °C until wpp and then shifted to 27.5 °C. Note the lack of precise alignment of neighboring hairs. (F) A micrograph of a *ptcGal4 Gal80^{ts}/UAS-DN-Rab11* pupal wing from a fly grown at 27.5 °C. The large arrow shows the boundary of the *ptc* domain (above inside). This image shows immunolocalization of Stan. The small arrow shows a cell with an increased level of improperly localized Stan. (G) A merge of F and H. (H) The same wing shown in F but showing F-actin staining in green. The asterisks are on abnormally shaped cells. (I) A micrograph of a *ptcGal4 Gal80^{ts}/UAS-DN-Rab11* pupal wing from a fly grown at 27.5 °C. The large arrow shows the boundary of the *ptc* domain (above inside). This image shows immunolocalization of In. Note the zigzag accumulation pattern for In outside of the *ptc* domain and the aberrant cell shape and In localization inside the *ptc* domain. (J) A merge of I and K. (K) The same wing as in I but showing F-actin staining. The asterisks are on abnormally shaped cells. (L) A 32 h *ptc-Gal/UAS-GFP-Rab11* pupal wing. (M) A merge of L and N. The arrow points to a cell where GFP-Rab11 is showing distal accumulation prior to F-actin accumulation. This shows that GFP-Rab11 is an earlier marker of hair outgrowth than F-actin. The arrowhead points to a cell where the hair is also marked by F-actin accumulation. (O) A 34 h *ptc-Gal/UAS-GFP-Rab11* pupal wing stained for GFP. (P) A merge of O and Q. (Q). A 34 h *ptc-Gal/UAS-GFP-Rab11* pupal wing stained for F-actin. (R) A 35 h *ap-Gal/UAS-GFP-Rab11* pupal wing imaged in vivo. The arrow points to the "blob" of GFP-Rab11 at the tip of the growing hair.

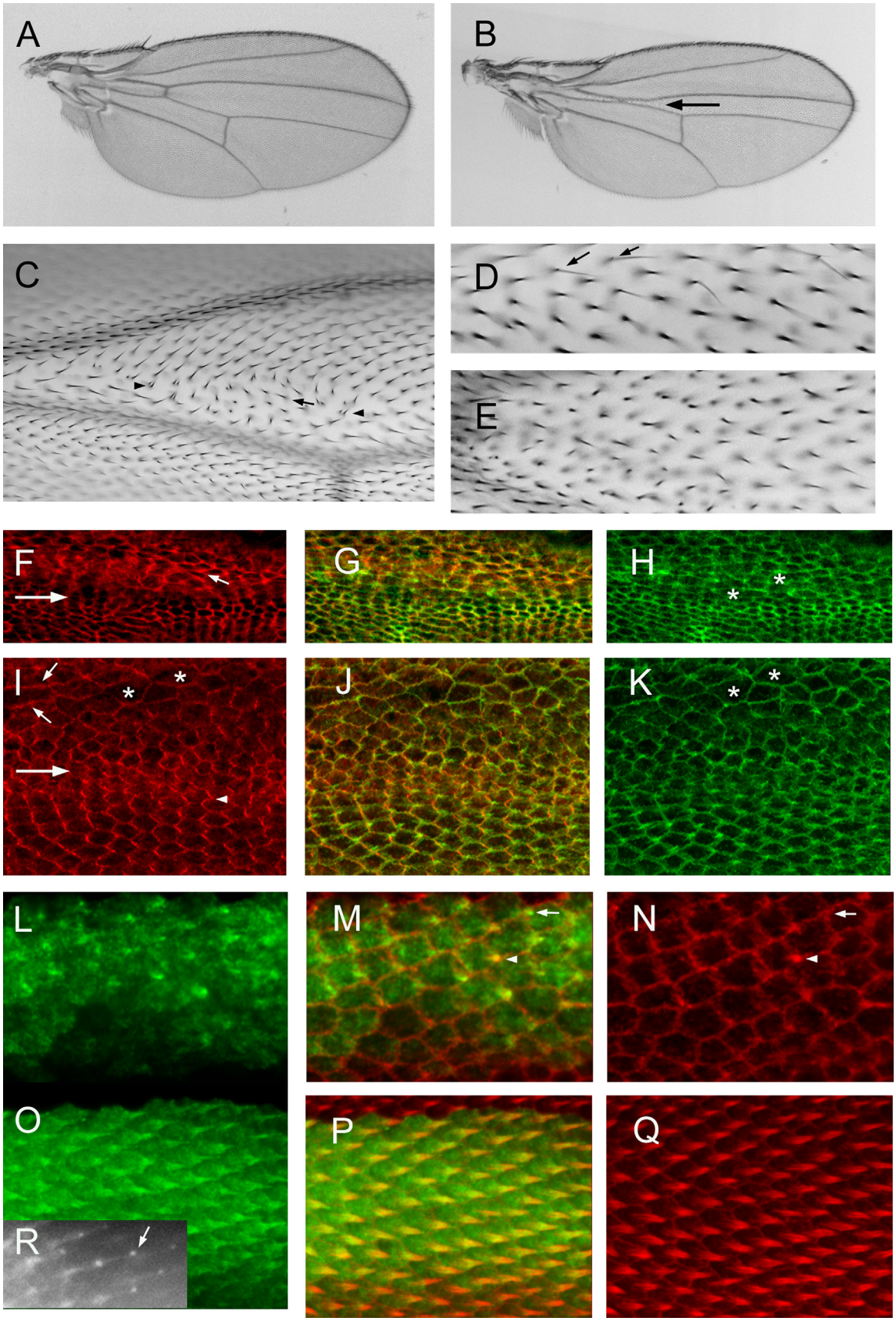
A
B
C
D
E
F
G
H
I
J
K
L
M
N
O
P
Q
R

network, and in some cases it appeared to outline cells (Fig. 2J–M, Fig. S5A, D, H). We also noticed that clone cells hair growth often appeared to be retarded and abnormal (Fig. 2J–M arrowhead). We also could detect abnormal hairs in nearby wild type cells, thus *dyl* oe can act cell non-autonomously ((Fig. 2J–M arrow, Fig. S5A–C arrows). This non-autonomy was usually associated with obvious non-autonomous Dyl accumulation.

Rab11 and hair morphogenesis

In developing bristles Dyl acts as a Rab11 effector for chitin deposition and Rab11 function is required for the plasma membrane localization of Dyl (Nagaraj and Adler, 2012). To determine if this relationship was conserved in hairs we attempted to determine if a lack of Rab11 function lead to a similar hair morphology phenotype. We did not see any phenotype associated with a kd of Rab11 in hairs. Nor did we see any hair phenotype in Rab11 hypomorphs that survived to adulthood and showed a mutant phenotype in macrochaetae. We also generated clones of wing cells that were homozygous for two independent Rab11 null alleles (Bogard et al., 2007; Dollar et al., 2002). We did not see any hair phenotype in such wings but a limitation of these experiments was that we only obtained small clones. A failure to recover Rab11 null clones in imaginal discs was reported recently (Xu et al., 2011) and is consistent with our observations. This could be due to Rab11 having an imaginal disc cell essential function (e.g. cytokinesis) and this function being more sensitive to a lack of Rab11 than Dyl insertion into the plasma membrane. This would result in cells with low levels of Rab11 being lost and explain our failure to see a Rab11 loss of function phenotype.

As an alternative to examining mutants in or a kd of the endogenous *Rab11* gene we examined the consequences of the expression of either a dominant negative (DN) or constitutively active (CA) Rab11. Driving the expression of DN-Rab11 mutant protein using *ptc-Gal4* was lethal. To get around this lethality we used a temperature sensitive Gal80 protein and a variety of temperature (shift) regimens. As a first check that the DN-Rab11 was able to induce a *Rab11* loss of function like phenotype we examined the scutellar bristles where *ptc-Gal4* drives transgene expression. *Rab11* is known to be essential for the determinative cell divisions that give rise to the bristle sense organ and for morphogenesis of the bristle shaft (Emery et al., 2005; Jafar-Nejad et al., 2005; Nagaraj and Adler, 2012). In flies that were raised at 27.5 °C (which allows a low level of expression in the presence of the ts Gal80 protein) several phenotypes were seen including a complete loss of the scutellar bristles, the loss of one or more but not all of the scutellar bristles and bristles that were short, or curved or mis-oriented. We also saw flies with extra scutellar bristles. In flies raised at 21 °C no bristle phenotype was observed. We thus concluded the expression of DN-Rab11 by *ptc-Gal4* was able to produce loss of function like phenotypes. In flies that were raised as larvae at 27.5 °C and then shifted to 29 °C at white prepuae the scutellum was greatly reduced in size suggesting that a high level of expression of DN-Rab11 either reduced cell proliferation or caused cell death (Fig. S6C).

When animals were grown at 29.5 °C (restrictive condition) most died prior to pupation although a small number of pupae were formed after 8–9 days of culture. None of these exceptional pupae eclosed as adults. A few made it to the pharate adult stage and these showed a variety of defects including legs that were truncated distally and/or proximally (Fig. S6A, B). When flies were grown at the permissive condition (21 °C) no mutant phenotype was detected on the wing (Fig. 5A, Table S1). In contrast, when they were grown at a semi-restrictive condition (27.5 °C) several phenotypes were seen and these were made more severe when the animals were shifted to 29.5 °C at white prepupae (wpp). Consistent with Rab11 functioning in growth, larvae grown at 27.5 °C had a reduction in the size of the *ptc* domain in the center of the wing (Fig. 5B). Along with this phenotype was a reduction or loss of the anterior cross vein. This "growth" function of Rab11 needs to be antagonized for a substantial period of time prior to 20 h awp for the phenotype to be manifested as it was suppressed when animals were shifted from 27.5 °C to 21 °C at wpp (Table S1). Further, flies raised at 21 °C and then shifted to 29 °C at wpp did not show a reduction in the size of the *ptc* domain. A second growth related phenotype was the appearance of occasional polypoid cells. Several other phenotypes were commonly seen in wings of flies raised at 27.5 °C. The most interesting was a PCP phenotype that resembled a loss of function in one or more of the genes of the *fz/stan* pathway (Fig. 5C). This was seen in most wings of flies grown at 27.5 °C. We immunolocalized two members of the *fz/stan* pathway in such pupal wings. We noticed that cells where DN-Rab11 was expressed most strongly were irregular in shape and had a larger cross section compared to the normal hexagonal cells (Fig. 5H, K). We detected an increase in Stan staining and a degradation of the normal zig zag pattern (Fig. 5F) (Usui et al., 1999). We also immunolocalized the downstream planar cell polarity effector protein Inturned (Adler et al., 2004). The normal zig zag accumulation of this protein along the proximal side of wing cells was similarly disrupted (Fig. 5I).

We also detected hair abnormalities that resembled those seen in *dyl*. These included thin, split, multipled, and very short hairs and hairs that were not well aligned with their neighbors (Fig. 5D, E). We also detected cuticle abnormalities in some wings. All of these phenotypes were seen in a small number of cells but in a substantial fraction of wings (Table S1). These were also seen when animals were shifted from 21 °C to 27.5 or 29.5 °C 20–24 h awp and thus represent a "late hair" phenotype. In other experiments we found that a reduction in *Rab11* gene dose (1 vs 2 functional copies) appeared to enhance the phenotypes seen with the expression of DN-Rab11. This observation supports the hypothesis that the effects of the DN-Rab11 were specific for normal *Rab11* functions. The presence of these *dyl* like phenotypes suggests that Dyl may be a Rab11 effector in hairs as well as bristles. We were unable to get compelling data on this point as we did not detect an alteration in Dyl localization after the expression of DN-Rab11 (data not shown). This seems likely to

Fig. 6. *kkv* and hair morphogenesis. (A) An SEM of an adult wing that contains a pair of small kkv^1 clones. These are outlined in white. (B) A higher mag image of part of A. The arrow points to a kkv^1 hair and the arrowhead to a neighboring wild type hair. Note how the kkv^1 is flaccid and fainter. However, it is not branched and is neither thinner nor shorter than wild type. (C) Shown is a bright field image of a region of an adult wing bearing two small kkv^1 clones. The arrow points to a faint kkv^1 hair and the arrowhead to a location where the faint mutant hair cannot be seen due to being out of the plane of focus. (D) A bright field micrograph of a *knk* clone (arrow). Note the similarity to the kkv^1 clone. (E) A region of a 34 h pupal wing stained for F-actin (red) that contains a kkv^1 clone. (F) The image from E showing the location of the clone as marked by the loss of GFP. (G) A region of a 44 h pupal wing stained for chitin (red) that contains a kkv^1 clone. (H) The image from G showing the location of the clone as marked by the loss of GFP. Note at this late stage GFP staining quality is lower than in younger wings. Note the bright spot of chitin staining at the base of the hairs. Note that chitin staining is lost in the clone cells showing the specificity of the chitin staining. (I) A region of a 34 h pupal wing stained for Dyl (red) that contains a kkv^1 clone. (J) The image from I showing the location of the clone as marked by the loss of GFP. Note that the hairs inside the clone do not show altered Dyl staining. (K) A kkv^1 clone inside of the *ptc* domain where *dyl* has been knocked down by RNAi. The arrow points to a faint and flaccid hair (hence one that is mutant for *kkv*) that shows dramatic branching. (L) A different focal plane from the same region of the same wing shown in K. The asterisk marks the location of the *kkv* clone cell. No hair is seen due to it laying on the wing blade surface.

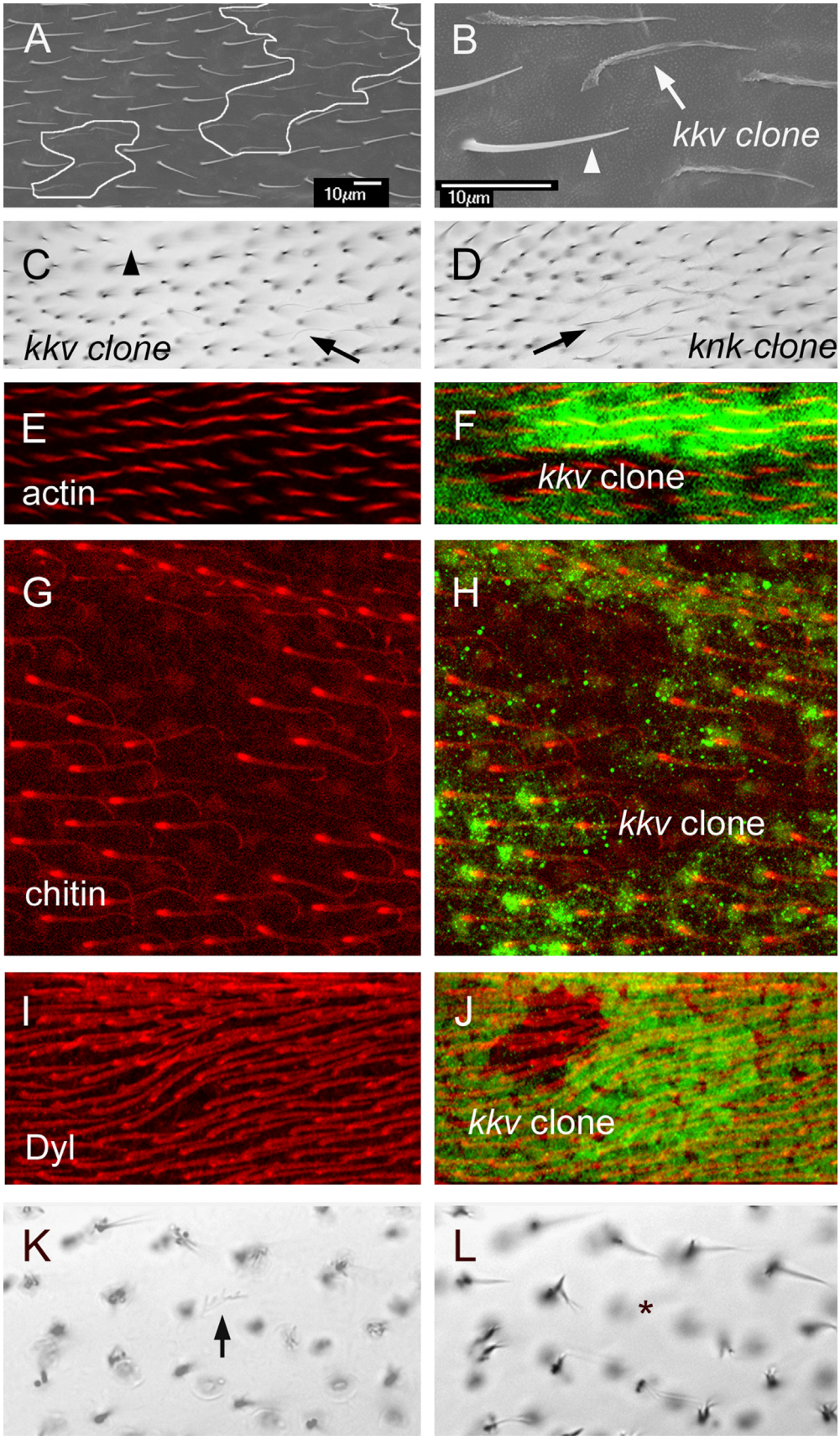
A
10μm
B
kkv clone
10μm
C
kkv clone
D
knk clone
E
actin
F
kkv clone
G
chitin
H
kkv clone
I
Dyl
J
kkv clone
K
L
*

be due to the very weak nature of the DN-Rab11 *dyl* like phenotype. Our results on the effects of expressing DN-RAb11 differ somewhat from those reported by Gault et al. (2012) who reported short, missing and deformed hairs in pupal wings. The experiments were done differently and this may have shifted the predominant phenotypes.

We also carried out experiments where we expressed constitutively active Rab11. As was reported recently (Gault et al., 2012; Purvanov et al., 2010) this led to distally pointing multiple hair cells (data not shown). We also detected polyploid cells after the expression of CA-Rab11, consistent with Rab11 functioning in cytokinesis in wing cells (Giansanti et al., 2007; Xu et al., 2011).

Rab11 Is a good hair reporter

We examined the subcellular distribution of Rab11 in pupal wing cells using a GFP-Rab11 reporter shown to be functional in bristle cells by a rescue assay (Nagaraj and Adler, 2012). Rab11 accumulated in growing hairs from the time of initiation (Fig. 5L–Q). Indeed it appeared to accumulate there earlier than F-actin, although that may simply be a reflection on the sensitivity of detection. In fixed cells we did not see evidence of enrichment at the distal tip of growing hairs as we had seen in growing bristles and laterals. However, in vivo imaging experiments showed preferential accumulation at the tip in what appeared as a small blob (Fig. 5R). It seems likely that the "blob" is not stable to fixation/dissection. At late stages in hair outgrowth (e.g. >38 h awp) it was clear that Rab11 was less abundant in the hair shaft and was concentrated around the base (Fig. S7B, C). That Rab11 accumulated in growing hairs was reported recently (Gault et al., 2012). During the process of hair elongation we observed an intracellular gradient of Rab11 across the apical region of the cell that deceased as one moved back from the base of the hair (Fig. S8). This could be an indication of there being an overall bias in intracellular trafficking needed to build the hair. We also examined Rab11 accumulation in wing cells mutant for the *mwh* gene. Such mutations result in each wing cell forming multiple hairs of abnormal polarity. Rab11 appeared to accumulate over a larger region of the cell at hair initiation and it accumulated in all of the multiple hairs produced in the mutant (Fig. S7E, F). The latter of these results were recently reported by Gault et al. (2012).

The dyl split hair phenotype is not due to a lack of chitin

As reported above a lack of *dyl* function results in abnormal chitin deposition. This was also seen in developing bristles (Nagaraj and Adler, 2012) and is also likely in developing denticles (Fernandes et al., 2010). To determine if a lack of chitin could be responsible for the *dyl* hair phenotypes we examined clones of cells that were homozygous for a null allele in *kkv* (kkv^1), which encodes the chitin synthase responsible for synthesizing exoskeleton cuticle chitin (Gagou et al., 2002; Moussian et al., 2005; Ostrowski et al., 2002). *kkv* null hairs were almost invisible on first inspection in the light microscope, however they were visible with careful examination (Fig. 6C). This is due to very limited pigmentation and to the hairs being flacid and lying close to the wing blade cuticle. We did not observe any evidence of hair branching as seen with a lack of *dyl* function. We previously reported similar results with a hypomorphic *kkv* allele (Ren et al., 2005). We also examined *kkv* clone bearing wings in the SEM. These images confirmed that the *kkv* hairs were flacid and established they had an irregular surface (Fig. 6A, B). They also confirmed that the *kkv* mutant hairs were neither shorter nor thinner than wild type hairs nor were the mutant hairs branched. Indeed, they often appeared slightly longer than wild type neighbors. We also did not see any evidence for the hair "cup" associated with the *dyl* kd. We conclude that the presence of chitin is not required for the maintenance of hair integrity and that the branching of *dyl* mutant hairs requires an alternative explanation.

Since the deposition of chitin is abnormal in *dyl* kd cells it remained possible that abnormal chitin and not a lack of chitin was involved in hair branching. To eliminate this possibility we generated *kkv* null clones in wings where *dyl* function was knocked down in the central but not peripheral regions of the wing (*ptc-Gal4* > *dyl RNAi*). *kkv* clones outside of the *ptc* domain had the same morphology seen previously (Fig. 6C). Clones within the *ptc* domain showed hairs that had the branching phenotype of *dyl* and the flacid unpigmented phenotype of *kkv* (Fig. 6K, L) (i.e. the phenotypes were additive). Thus, chitin appears to be unrelated to the *dyl* hair branching phenotype.

We also examined marked *kkv* clones in the pupal wing. We first examined clones in older wings (>40 h apf) by chitin staining. As expected chitin staining was lost in the clone cells (Fig. 6G, H). This also served as a control for the specificity of our chitin staining protocol. Further, we did not see any effect on hair morphology as revealed by F-actin staining during outgrowth (Fig. 6E, F).

We next asked if the localization of Dyl to the hair requires the presence of chitin. To do this we immunolocalized Dyl in wings that contained marked kkv^1 clones. We did not detect any alteration in Dyl in clone cells (Fig. 6I, J), thus Dyl localization is independent of the presence of chitin.

A screen for additional genes that function along with dyl and kkv in hair morphogenesis

The *dyl* and *kkv* genes are notable in that their expression is highly modulated during wing development. We previously characterized the mRNA populations at three times in pupal wing development (Ren et al., 2005). At 24 h awp, around the time when cell division ceases, at 32 h awp the time of hair initiation and at 40 h around the time wing expansion and chitin deposition start. We found that several of the genes identified in this way had dramatic wing hair phenotypes. These included *kkv*, *knk* and *sha*. The results described above allow us to add *dyl* to this group. To try to identify other genes that worked with *dyl* and *kkv* in hair morphogenesis we carried out a small directed RNAi screen. We screened 107 genes whose wing expression increased at 32 and/or 40 h, or that were identified on FlyBase (McQuilton et al., 2012) as having an overall gene expression profile that was similar to *dyl* or *kkv*. A number of genes fit more than one criterion. Included are several genes that fit these criteria and were known prior to the screen to have a hair phenotype (e.g *pawn* (Arruda and Dolph, 2003) and *shaven baby* (Delon et al., 2003). In the screen we used a directed kd of the gene using transgene induced RNAi. Knockdowns of 47 of the genes produced a mutant phenotype that was reminiscent of one or more of the phenotypes seen with *dyl* or *kkv* (Table 1). In addition to *dyl* we found nine genes that gave split hairs, 17 that resulted in thin hairs, 16 that resulted in misaligned neighboring hairs and two that produced hair cups. In addition to *kkv* and *knk* we identified three additional genes where a kd resulted in faint hairs. In our screen we noticed a new phenotype that was similar in some ways to the *kkv* and *dyl* phenotypes but distinct from both. We first clearly identified it in knockdowns of the *ectodermal* (*ect*) gene. It was characterized by a somewhat faint and usually curved hair with a very faint and flacid base (Fig. 7E). In addition to *ect*, a kd of seven other genes gave this phenotype.

One gene that stood out was *Chitinase6* (*Cht6*), as the kd resulted in a weak version of all of the *dyl* phenotypes (Fig. 7A–D). This makes it a strong candidate for a gene that works along with *dyl* in hair morphogenesis. That the *Cht6* phenotypes were so much weaker could be due to the kd being less effective for *Cht6*,

Table 1
Genes that showed a hair phenotype.

Gene	RNAi line or mutant	Split hairs (*dyl*-like)	Thin hairs (*dyl*-like)	Faint hairs (*kkv*-like)	*ect* like hairs	Hair cup (*dyl*-like)	Misaligned hairs	Cuticle defects	Reason for screening[a]	Comment
dyl (*CG15013*)	V102166 V39022 V39023 dyl^{MI}	+++	+++			++	+++	+	32, 40, d, l, m	ZP domain
Cht6 (*CG43374*)	V107916 V38886	+	++			+	++	+/−	40, l	Chitinase
ect (*CG6611*)	V104650	+			++		+	+	32, 40, d, m	
CG15020	V101086				+/−			+	32, d	ZP domain
Cyp301a1 (*CG8587*)	V109771 V26989	+/−							40, d	Curved hairs
kkv (*CG2666*)	kkv^{1} V100327			+++				+	40, k, l	Chitin synthase1
knk (*CG6217*)	knk^{f01902} V106302			+++				+	40, k, l	Chitin stability
CG5873	V14374		+		+				40, k	Heme peroxidase
mtg (*CG7549*)	V108951							+	32, d, l, m	Chitin binding
CG15211	V104929			+	+			+	32, 40	MARVEL domain
cyr (*CG15335*)	V28555						+/−		32, 40, m	ZP domain
uif (CG9138)	V101153							+	32, 40	Lectin, EGF domain
mey (*CG12063*)	V106568				+/−				32, m	ZP domain
CG12206	V14558		+/−				+/−		32	
ed (*CG12676*)	V104279 V27044		+					+	32	Cell-cell adhesion
CG30463	V4923		+/−						32	Glycosyltransferase Ricin B lectin
Rab23 (*CG2108*)	T28025		+						32, l	Multiple hair cells
sha (*CG13209*)	V36512 Several alleles	+	++						32, l, m	Localizes to growing hairs
CG10933	V104282						+		32	Src homology 3 domain
svb (CG6824)	V41584		+++	++	+		+	+	32, l	Transcription factor
CG3036	V108500							+	40	MFS transporter family
CG16953	V109873							++	40	
CG14770	V106550		+/−						40	
Cpr97Eb (*CG15884*)	V19545						+/−	+/−	40	Cuticle protein
Cpr49Ah (*CG8515*)	V23183		+/−				+/−		40	Cuticle protein
Eip71CD (*CG7266*)	V26009						+/−		40	Methionine-(S)-S-oxide reductase
CG13917	V32082	+/−				+		++	40	BTB/POZ
karst (CG12008)	V37074						+/−		40	βH-spectrin
UGP (CG4347)	V109632	+ b	+				+/−	+	40	UTP:glucose-1-phosphate uridylyltransferase
pwn (*CG11101*)	V101282 pwn^{1}	+/− b	+++						d, l, m	EGF domains
dy (*CG9355*)	V102255 dy^{1}							+++	d, l	ZP domain
CG15740	V107087		+/−				+		d, m	
CG42331	V104585						+/−	+	d	Peroxidase
m (*CG9369*)	V8036 m^{1}, m^{D}	++	+				+	+++	d, m	ZP domain
CG9095	V104608		+ tip				+		d, m	C type lectin
CG43366	V101186		+/−						d	Endopeptidase inhibitor
CG14107	V102232		+/−					+	d, m	
CG6347	V101253						+		d	Peptidase
CG15080	V106073							+	d	
CG15017	V103326							+/−	d	
CG31559	V33967	+				+/−		+/−	d, m	
CG13188	V102370			+					k	Smad domain
CG10232	V100033				+		+		d	Peptidase
CG1869	V104445				+/−			+/−	k	Chitinase 7
Syn1 (*CG7152*)	V104992		+/−		+/−				k	
TwdlE (*CG14534*)	V107483				+/−				k	

40—Increased expression at 40 h awp—from Ren et al. (2005).
d—Expression similar to *dyl*—FlyBase—McQuilton et al. (2012).
k—Expression similar to *kkv*—Flybase—McQuilton et al. (2012).
m—mE2 34 mRNA expression cluster 07—ModEncode—FlyBase.
l—Literature.

[a] 32—Increased expression at 32 h awp—from Ren et al. (2005).

to *Cht6* being relatively less important for hair morphogeneis or to *Cht6* being partially redundant with one or more unknown genes (e.g. other chitinases). The relative weakness of the *Cht6* vs *dyl* kd complicated efforts to examine the relationship between the two genes. For example, we did not see a clear alteration in *dyl* immunostaining in the *Cht6* kd but the significance of that is not clear as the vast majority of hairs are completely normal in such a wing. We identified several genotypes and wing regions where

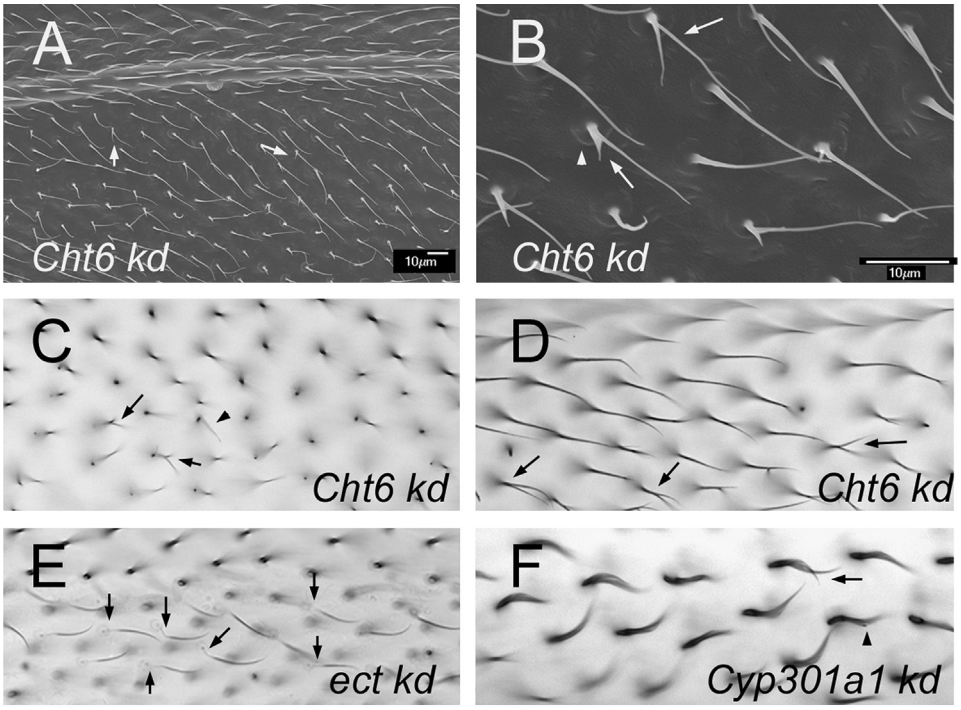

Fig. 7. (A) An SEM of an adult *ptc-Gal4 UAS-Cht6 RNAi* wing. Arrows point to branched hairs. Note the poor alignment of neighboring hairs. (B). A higher magnification image of a region of A. The arro points to a split hair. The arrowhead points to a "cup" at the base of the hair. (C). A brightfield micrograph of an adult *ptc-Gal4 UAS-Cht6 RNAi* wing. The arrows point to branched and thin hairs. (D). A brightfield micrograph of an adult *ptc-Gal4 UAS-Cht6 RNAi* wing. The arrows point to branched hairs. (E). A brightfield micrograph of an adult *ptc-Gal4 UAS-ect RNAi* wing. The arrows point to hairs that show the "*ect*" phenotype of hairs with a faint and wimpy proximal region. (F). A brightfield micrograph of an adult *ptc-Gal4 UAS-Cyp301a RNAi* wing. The arrows point to split hairs. Note the curved shape of all hairs in this wing region.

there was a weak *dyl* kd phenotype and we then assessed the phenotype in the *dyl*, *Cht6* double kd. The clearest results were seen by examining the dorsal surface of the wing just distal to the posterior cross vein (from the vein to five cells distal). About 1/2 of *vg-Gal4/UAS-dyl-RNAi* wings did not show a phenotype in this region, while the others showed a small number of hairs with the thin and or split phenotype characteristic of *dyl*. On average we found 1.6 (sd 2.1) such hairs per wing region. No phenotype was seen in *vg-Gal4/UAS-Cht6-RNAi* wings in the same location. In contrast in the double kd (*UAS-dyl-RNAi vg-Gal4/UAS-Cht6-RNAi*) all wings showed a phenotype with a mean of 10.5 (sd 4.6) *dyl* like hairs per wing region. This difference was highly significant ($p=5\times10^{-5}$ (*t* test comparing *UAS-dyl-RNAi vg-Gal4* vs *UAS-dyl-RNAi vg-Gal4/UAS-Cht6-RNAi*). Thus, in this sensitized situation we saw an interaction that indicated the two genes functioned in an additive way. We also examined *UAS-dicer2*; *ptc-Gal4/Cht6-RNAi* pupal wings by Dyl immunostaining but we did not detect any changes in the accumulation of Dyl. This could be due to the weakness of the *Cht6* kd or to Dyl accumulation not being sensitive to *Cht6* function. A way to obtain a stronger *Cht6* loss of function will be needed to resolve this issue.

Several of the other genes identified are worth noting. The *shaven baby* transcription factor was previously reported to be important for hair morphogenesis and we confirmed those results (Delon et al., 2003). A kd of a second likely transcription factor, CG13188, which encodes a Smad protein gave a faint hair phenotype that appeared to be a weak version of the *kkv* phenotype. Knockdowns of other ZP domain proteins gave a range of hair and wing blade phenotypes consistent with the results seen for this family of proteins in embryonic denticle morphogenesis and cuticle deposition (Fernandes et al., 2010). None of these were as severe as the *dyl* kd with regard to hair morphology. Several genes that encode cuticle proteins or cuticle binding proteins also gave hair phenotypes. These included *Cht6*, *kkv*, *knk*, *mtg*, *Cpr97Eb*, *Cpr49Ah* and *Cht7*. One of the most interesting and surprising phenotypes was seen with kd of *Cyp301a1*. This member of the cytochrome P450 family was screened because its expression increased at 40 h and its overall expression pattern was similar to *dyl*. It is listed in Table 1 due to it causing split hairs but its most prominent phenotype was a curvy hair (Fig. 7F). This was also seen in bristles (data not shown). We do not consider the failure to see a wing hair phenotype in the other 60 genes screened (Table S2) to be particularly informative. Our results could be due to the genes not functioning in hair morphogenesis, due to the genes being functionally redundant or to the knock downs not being effective enough to see a phenotype.

Discussion

Dyl and actin

Previous studies have implicated Dyl and other ZP domain proteins in linking the cuticle to the plasma membrane and in the patterned deposition of chitin (Fernandes et al., 2010; Nagaraj and Adler, 2012). Other studies suggested that it could regulate the cytoskeleton (Bokel et al., 2005; Brodu et al., 2010; Roch et al., 2003). Our finding premature hair initiation in *dyl* kd wing cells establishes that *dyl* regulates the cytoskeleton and suggests the possibility that Dyl negatively regulates the actin cytoskeleton prior to hair initiation. At later stages in hair morphogenesis the situation is more complicated. In older kd cells we observed an increase in the accumulation of F-actin in the basal cup but a decrease in hair F-actin. The decrease in the hair could be due to a role for Dyl in promoting F-actin accumulation there and the increase in the basal disc could be due to a displacement of F-actin from the hair. The evidence for possibly increased hair F-actin with oe *dyl* is consistent with this possibility. Alternatively, the increased F-actin in the basal disc could be due to Dyl normally negatively regulating actin polymerization there. Regardless of the

mechanism involved the effects on the actin cytoskeleton are stage and site specific arguing that Dyl does not act as a general actin regulator. Other observations were consistent with that hypothesis. For, example we did not see any alteration in F-actin staining associated with a kd of *dyl* in wing discs or young pupal wings (data not shown). In contrast, mutations in genes that encode proteins that are key general components in the regulation of F-actin such as cofilin (*tsr*) and *AIP1* (*flr*) lead to enormous increases in F-actin levels and increased F-actin stability (Gunsalus et al., 1995; Ren et al., 2007) in a variety of cell types at all stages of development. Further evidence against Dyl functioning as a general regulator of the actin cytoskeleton is the nature of the *dyl* hair phenotype. For example, mutations in the F-actin bundling protein genes *forked* and *singed* (Cant et al., 1994; Petersen et al., 1994; Tilney et al., 1995), in non-muscle myosin encoding genes such as *crinkled* (Kiehart et al., 2004) or *zipper* (Franke et al., 2010), in regulators such as Rho kinase (Winter et al., 2001) and in F-actin depolymerizing protein encoding genes such as *twin star* (Gunsalus et al., 1995) and *flare* (Ren et al., 2007) all result in hair phenotypes. The phenotypes associated with these classes of genes are distinct from one another and from that of *dyl*. Thus, it seems unlikely the *dyl* mutant phenotype is mediated by effects on actin bundling, polymerization state or myosin related functions. We suggest that Dyl and perhaps other ZP domain proteins regulate the actin cytoskeleton by assembling and locally concentrating a mix of actin regulators.

The vast majority of the Dyl protein is predicted to be extracellular with only the C terminal 15 amino acids predicted to be cytoplasmic (Plaza et al., 2010). This region of the protein could function directly in the regulation of the actin cytoskeleton, however the sequence does not contain similarity to known actin regulators. This segment of the protein is very highly conserved in other Drosophila species, as is the entire Dyl protein, suggesting it is of functional importance, although in comparisons to Dyl homologs in more distant insects it is not the most highly conserved region. This segment is positively charged (five positively charged residues compared to a single negatively charged one) thus it might interact with the negatively charged phosphate groups of membrane lipids and in this way indirectly signal to the actin cytoskeleon (Shewan et al., 2011; Zhao et al., 2010). An alternative explanation is that the extracellular domain interacts with one or more proteins in the extracellular space that then signal back to the cytoplasm to regulate the actin cytoskeleton. This hypothesis could explain the non-autonomous hair defects associated with *dyl* oe.

The Dyl protein contains a potential consensus furin cleavage site (RRRR aa 499–502) (Roch et al., 2003) located in its large putative extracellular domain. Hence it is possible that most of the Dyl protein is completely extracellular rather than being part of an integral membrane protein (Plaza et al., 2010). Given the possible cleavage site it is a bit surprising that we found strict cell autonomy in *dyl* kd flip out clones. Consistent with Dyl being cleaved we observed oe Dyl beyond the borders of flip out clones. To explain this set of observations we suggest that under normal expression conditions Dyl is either protected from cleavage by a binding partner or that the cleaved protein remains connected to the synthesizing cell. This could be a consequence of binding to the extracellular domain of another transmembrane protein. In either case the Dyl binding partner could share the highly modulated *dyl* expression profile. When *dyl* is expressed constitutively in the flip out clone cells the binding partner would not be present. Hence, Dyl would be cleaved and able to migrate to produce the non-autonomous accumulation observed.

The over expressed Dyl protein appeared fibrous consistent with previous observations that ZP domain proteins polymerize and can form fibrous structures (Plaza et al., 2010). Our observation may be useful in establishing an in vivo assay for fiber assembly by ZP domain proteins. It will be interesting to see if other ZP domain proteins will form such fibrous structures when expressed in the pupal wing or if there are gene specific factors that are needed. Why there appeared to be a distal bias to the non-autonomous accumulation is unclear. Further experimentation will be required to determine if, when and how Dyl is cleaved.

The dyl PCP phenotype Is unique

The abnormal polarity of wing hairs in *dyl* mutants represents a novel planar cell polarity (PCP) phenotype. It differs in many ways from those seen in *fz/stan* and *ds/ft* in that it does not alter polarity at early stages of hair outgrowth; rather it results from a failure to maintain normal PCP. Further, it does not result in extensive swirling of mutant hairs as in *dyl* neighboring hairs are often not well aligned with one another (Adler, 2002, 2012; Goodrich and Strutt, 2011; Lawrence et al., 2007; Wu and Mlodzik, 2009). Those same general characteristics have been seen with mutations in septate junction components (Moyer and Jacobs, 2008; Venema et al., 2004) but in those mutations the abnormal polarity is associated with the hair base/pedestal being tilted with respect to the surface of the wing blade. That is not the case for *dyl*. Hence, *dyl* and likely *Cht6* appear to be openings into a new mechanism for maintaining hair polarity on the fly wing. We suggest that this involves the cuticle acting as a "glove" to maintain the orientation of hairs as wing cells go through their later steps in wing morphogenesis (Mitchell et al., 1990; Roch et al., 2003). These steps, which have not been intensively studied in recent years include cell flattening, the formation of the hair pedestal and the movement of the hair to the central region on the apical surface of the cell.

Rab11 and Dyl in hairs

During bristle morphogenesis Rab11 is required for the plasma membrane localization of Dyl (Nagaraj and Adler, 2012). Mutants for either of these genes give rise to a bristle "stub" phenotype due to collapse of the bristle that appears to be a consequence of a failure to secrete a patterned and organized cuticle. Although we observed an analogous phenotype for *dyl* in wing hairs we did not detect any wing hair phenotypes in *Rab11* null mutant clones or after a *Rab11* kd. However, we found *Rab11* to accumulate at the site of hair outgrowth, in growing hairs and preferentially in blobs at the tips of growing hairs. These localization patterns are reminiscent of that in bristles and arista laterals where Rab11 is functionally important (Nagaraj and Adler, 2012) and suggest the lack of a mutant phenotype in hairs is due to redundancy or to other cell essential functions being more sensitive to a loss of Rab11. Consistent with these possibilities the expression of either dominant negative or constitutively active Rab11 leads to a range of hair phenotypes including mimics of the *dyl* hair phenotype. Another was a planar cell polarity phenotype typical of mutations in the *fz/stan* pathway genes. We found this was associated with both abnormal cell shape and a disruption in the normal zig zag accumulation of the *fz/stan* pathway proteins Stan and In at the distal/proximal sides of pupal wing cells (Adler et al., 2004; Usui et al., 1999). This result was unexpected as previous results from Strutt and Strutt (2008) implicated Rab4 and not Rab11 in the endosomal trafficking of Stan and Fz. They found that Stan co-localized with Rab4 and Rab5 but not with Rab11. However, the authors could not rule out Rab11 taking over in the absence of Rab4 function. They found the expression of DN-Rab11 to be toxic (as we have) but did not report any effects on PCP. It is unclear if DN-Rab11 directly interfered with the intracellular trafficking involved in the formation of the proximal and distal protein

complexes that contain *fz/stan* pathway components. The effects could be indirect, for example, due to the abnormal cell shape or to defects in the trafficking of other components.

We suspect that bristle cells are more sensitive than hairs to a loss of Rab11 function and that this is due to their much greater length. An observation consistent with this hypothesis is that a Rab11 hypomorph produces a bristle morphology phenotype that is obvious in the largest bristles (thoracic macrochaetae) but not in smaller bristles or in hairs. The largest bristles were also far more sensitive to a Rab11 kd than shorter bristles (Nagaraj and Adler, 2012). This could be due to Rab11 being important for long-range intracellular transport while other pathways might suffice for shorter distances.

Chitin is not the only target of dyl

Drosophila ZP domain proteins as a group have been implicated in cuticle assembly (see for example (Fernandes et al., 2010; Nagaraj and Adler, 2012; Roch et al., 2003)). Here we established that while *dyl* is required for normal chitin deposition, chitin is not required for normal Dyl accumulation. Thus, Dyl appears to function upstream of chitin in cuticle assembly. We suggest this will be true for other ZP domain proteins.

It is striking that both the *dyl* bristle and hair mutant phenotypes are associated with defects after outgrowth. We found defects in chitin deposition in *dyl* mutant hairs much as we previously found in bristles (Nagaraj and Adler, 2012). The range of bristle phenotypes seen in *kkv* mutants overlapped but was weaker on average than that seen in *dyl* mutants, which lead us to argue that Dyl had functions other than organizing chitin deposition (Nagaraj and Adler, 2012). More compelling data was obtained studying wing hairs where the mutant phenotypes are distinctly different and additive. Thus a defect in chitin deposition cannot explain the *dyl* mutant phenotype. It seems likely that other targets of Dyl are important for maintaining hair structure. Obvious candidates include cuticle proteins, cuticle interacting proteins and the actin cytoskeleton. Due to the large number of putative cuticle proteins encoded in the Drosophila genome it is not obvious which ones might be important in hairs. Further the large number of such genes suggests the possibility that they will be redundant making it difficult to obtain convincing functional data. Nonetheless it is interesting that knockdowns of several cuticle proteins produced hair phenotypes, albeit weak ones. These are certainly good candidates for being possible Dyl targets. Our finding that a knock down of *Cht6* could mimic all of the hair morphology phenotypes seen in adult *dyl* hairs is strong support for the idea that the adult hair phenotypes are a result of a defect in cuticle formation and it could be a Dyl target.

As noted above, Dyl appears to regulate the actin cytoskeleton in hair forming cells. It is possible that the late hair morphology abnormalities associated with a lack of *dyl* function are due to effects on the cytoskeleton and not to effects on cuticle deposition. Such an explanation is not tenable for the similar bristle collapse phenotype as no defects in F-actin organization were seen in that cell type. Thus, by analogy we think it unlikely that most or all of the *dyl* mutant hair phenotype is due to effects on the cytoskeleton. Further, many mutations are known that alter the function of the actin cytoskeleton and none have been found to produce a mutant hair or bristle phenotype due to collapse.

The function of Cyp301a1

Published data suggested that *Cyp301a1* may function in the metabolism of ecdysone and in the formation of cuticle (Sztal et al., 2012). The increase in expression of *Cyp301a1* around the time of the start of wing cuticle deposition is consistent with that suggestion. However, the wing hair phenotype we found fits better with an alternative mechanism. The curved hair and bristle phenotypes are reminiscent of phenotypes associated with mutations in genes that regulate the actin cytoskeleton such as *singed* and *forked* that bundle F-actin (Tilney et al., 1995). We suggest that *Cyp301a1* may function in the regulation of the cytoskeleton. There is little evidence in the literature for P450s regulating the cytoskeleton so it is difficult to guess as to a possible mechanism. We note that recently the Mical protein, which contains redox activity, is a potent regulator of actin dynamics in flies (Hung et al., 2010). Hence, novel mechanisms for regulating the cytoskeleton continue to be discovered.

Acknowledgments

This work was supported by a Grant from the NIGMS to pna and an ARRA supplement to that grant. We thank our colleagues in the fly community for generously sharing reagents.

Appendix A. Supporting information

Supplementary data associated with this article can be found in the online version at http://dx.doi.org/10.1016/j.ydbio.2013.04.012.

References

Adler, P.N., 2002. Planar signaling and morphogenesis in Drosophila. Dev. Cell 2, 525–535.
Adler, P.N., 2012. The frizzled/stan pathway and planar cell polarity in the Drosophila wing. Curr. Top. Dev. Biol. 101, 1–31.
Adler, P.N., Charlton, J., Liu, J., 1998. Mutations in the cadherin superfamily member gene dachsous cause a tissue polarity phenotype by altering frizzled signaling. Development 125, 959–968.
Adler, P.N., Zhu, C., Stone, D., 2004. Inturned localizes to the proximal side of wing cells under the instruction of upstream planar polarity proteins. Curr. Biol. 14, 2046–2051.
Amonlirdviman, K., Khare, N.A., Tree, D.R., Chen, W.S., Axelrod, J.D., Tomlin, C.J., 2005. Mathematical modeling of planar cell polarity to understand domineering nonautonomy. Science 307, 423–426.
Arruda, S.E., Dolph, P.J., 2003. Molecular cloning of the pawn locus from *Drosophila melanogaster*. Gene 310, 169–173.
Bogard, N., Lan, L., Xu, J., Cohen, R.S., 2007. Rab11 maintains connections between germline stem cells and niche cells in the Drosophila ovary. Development 134, 3413–3418.
Bokel, C., Prokop, A., Brown, N.H., 2005. Papillote and Piopio: Drosophila ZP-domain proteins required for cell adhesion to the apical extracellular matrix and microtubule organization. J. Cell Sci. 118, 633–642.
Brodu, V., Baffet, A.D., Le Droguen, P.M., Casanova, J., Guichet, A., 2010. A developmentally regulated two-step process generates a noncentrosomal microtubule network in Drosophila tracheal cells. Dev. Cell 18, 790–801.
Cant, K., Knowles, B.A., Mooseker, M.S., Cooley, L., 1994. Drosophila singed, a fascin homolog, is required for actin bundle formation during oogenesis and bristle extension. J. Cell Biol. 125, 369–380.
Delon, I., Chanut-Delalande, H., Payre, F., 2003. The Ovo/Shavenbaby transcription factor specifies actin remodelling during epidermal differentiation in Drosophila. Mech. Dev. 120, 747–758.
Devine, W.P., Lubarsky, B., Shaw, K., Luschnig, S., Messina, L., Krasnow, M.A., 2005. Requirement for chitin biosynthesis in epithelial tube morphogenesis. Proc. Natl. Acad. Sci. USA 102, 17014–17019.
Dollar, G., Struckhoff, E., Michaud, J., Cohen, R.S., 2002. Rab11 polarization of the Drosophila oocyte: a novel link between membrane trafficking, microtubule organization, and oskar mRNA localization and translation. Development 129, 517–526.
Emery, G., Hutterer, A., Berdnik, D., Mayer, B., Wirtz-Peitz, F., Gaitan, M.G., Knoblich, J.A., 2005. Asymmetric Rab 11 endosomes regulate delta recycling and specify cell fate in the Drosophila nervous system. Cell 122, 763–773.
Fernandes, I., Chanut-Delalande, H., Ferrer, P., Latapie, Y., Waltzer, L., Affolter, M., Payre, F., Plaza, S., 2010. Zona pellucida domain proteins remodel the apical compartment for localized cell shape changes. Dev. Cell 18, 64–76.
Franke, J.D., Montague, R.A., Kiehart, D.P., 2010. Nonmuscle myosin II is required for cell proliferation, cell sheet adhesion and wing hair morphology during wing morphogenesis. Dev. Biol. 345, 117–132.

Gagou, M.E., Kapsetaki, M., Turberg, A., Kafetzopoulos, D., 2002. Stage-specific expression of the chitin synthase DmeChSA and DmeChSB genes during the onset of Drosophila metamorphosis. Insect Biochem. Mol. Biol. 32, 141–146.
Gangishetti, U., Breitenbach, S., Zander, M., Saheb, S.K., Muller, U., Schwarz, H., Moussian, B., 2009. Effects of benzoylphenylurea on chitin synthesis and orientation in the cuticle of the Drosophila larva. Eur. J. Cell Biol. 88, 167–180.
Gault, W.J., Olguin, P., Weber, U., Mlodzik, M., 2012. Drosophila CK1-gamma, gilgamesh, controls PCP-mediated morphogenesis through regulation of vesicle trafficking. J. Cell Biol. 196, 605–621.
Geng, W., He, B., Wang, M., Adler, P.N., 2000. The tricornered gene, which is required for the integrity of epidermal cell extensions, encodes the Drosophila nuclear DBF2-related kinase. Genetics 156, 1817–1828.
Giansanti, M.G., Belloni, G., Gatti, M., 2007. Rab11 is required for membrane trafficking and actomyosin ring constriction in meiotic cytokinesis of Drosophila males. Mol. Biol. Cell 18, 5034–5047.
Goodrich, L.V., Strutt, D., 2011. Principles of planar polarity in animal development. Development 138, 1877–1892.
Gunsalus, K.C., Bonaccorsi, S., Williams, E., Verni, F., Gatti, M., Goldberg, M.L., 1995. Mutations in twinstar, a Drosophila gene encoding a cofilin/ADF homologue, result in defects in centrosome migration and cytokinesis. J. Cell Biol. 131, 1243–1259.
He, B., Adler, P.N., 2001. Cellular mechanisms in the development of the Drosophila arista. Mech. Dev. 104, 69–78.
He, Y., Fang, X., Emoto, K., Jan, Y.N., Adler, P.N., 2005. The tricornered Ser/Thr protein kinase is regulated by phosphorylation and interacts with furry during Drosophila wing hair development. Mol. Biol. Cell 16, 689–700.
Hung, R.J., Yazdani, U., Yoon, J., Wu, H., Yang, T., Gupta, N., Huang, Z., van Berkel, W.J., Terman, J.R., 2010. Mical links semaphorins to F-actin disassembly. Nature 463, 823–827.
Jafar-Nejad, H., Andrews, H.K., Acar, M., Bayat, V., Wirtz-Peitz, F., Mehta, S.Q., Knoblich, J.A., Bellen, H.J., 2005. Sec15, a component of the exocyst, promotes notch signaling during the asymmetric division of Drosophila sensory organ precursors. Dev. Cell 9, 351–363.
Kiehart, D.P., Franke, J.D., Chee, M.K., Montague, R.A., Chen, T.L., Roote, J., Ashburner, M., 2004. Drosophila crinkled, mutations of which disrupt morphogenesis and cause lethality, encodes fly myosin VIIA. Genetics 168, 1337–1352.
Lawrence, P.A., Struhl, G., Casal, J., 2007. Planar cell polarity: one or two pathways? Nat. Rev. Genet. 8, 555–563.
McQuilton, P., St. Pierre, S., Thurmond, J., Consortium, F., 2012. FlyBase 101—the basics of navigating FlyBase. Nucl. Acids Res. 40, D706–714.
Mitchell, H.K., Edens, J., Petersen, N.S., 1990. Stages of cell hair construction in Drosophila. Dev. Genet. 11, 133–140.
Moussian, B., Schwarz, H., Bartoszewski, S., Nusslein-Volhard, C., 2005. Involvement of chitin in exoskeleton morphogenesis in *Drosophila melanogaster*. J. Morphol. 264, 117–130.
Moyer, K.E., Jacobs, J.R., 2008. Varicose: a MAGUK required for the maturation and function of Drosophila septate junctions. BMC Dev. Biol. 8, 99.
Nagaraj, R., Adler, P.N., 2012. Dusky-like functions as a Rab11 effector for the deposition of cuticle during Drosophila bristle development. Development 139, 906–916.
Ostrowski, S., Dierick, H.A., Bejsovec, A., 2002. Genetic control of cuticle formation during embryonic development of *Drosophila melanogaster*. Genetics 161, 171–182.
Petersen, N.S., Lankenau, D.H., Mitchell, H.K., Young, P., Corces, V.G., 1994. Forked proteins are components of fiber bundles present in developing bristles of *Drosophila melanogaster*. Genetics 136, 173–182.
Plaza, S., Chanut-Delalande, H., Fernandes, I., Wassarman, P.M., Payre, F., 2010. From A to Z: apical structures and zona pellucida-domain proteins. Trends Cell Biol. 20, 524–532.
Price, M.H., Roberts, D.M., McCartney, B.M., Jezuit, E., Peifer, M., 2006. Cytoskeletal dynamics and cell signaling during planar polarity establishment in the Drosophila embryonic denticle. J. Cell Sci. 119, 403–415.
Purvanov, V., Koval, A., Katanaev, V.L., 2010. A direct and functional interaction between Go and Rab5 during G protein-coupled receptor signaling. Sci. Signal. 3, ra65.
Ren, N., Charlton, J., Adler, P.N., 2007. The flare gene, which encodes the AIP1 protein of Drosophila, functions to regulate F-actin disassembly in pupal epidermal cells. Genetics 176, 2223–2234.
Ren, N., Zhu, C., Lee, H., Adler, P.N., 2005. Gene expression during Drosophila wing morphogenesis and differentiation. Genetics 171, 625–638.
Roch, F., Alonso, C.R., Akam, M., 2003. Drosophila miniature and dusky encode ZP proteins required for cytoskeletal reorganisation during wing morphogenesis. J. Cell Sci. 116, 1199–1207.
Shewan, A., Eastburn, D.J., Mostov, K., 2011. Phosphoinositides in cell architecture. Cold Spring Harb Perspect. Biol. 3, a004796.
Struhl, G., Basler, K., 1993. Organizing acitivity of wingless protein in Drosophila. Cell 72, 527–540.
Strutt, D., 2002. The asymmetric subcellular localisation of components of the planar polarity pathway. Sem. Cell Dev. Biol. 13, 225–231.
Strutt, H., Strutt, D., 2008. Differential stability of flamingo protein complexes underlies the establishment of planar polarity. Curr. Biol.: CB 18, 1555–1564.
Sztal, T., Chung, H., Berger, S., Currie, P.D., Batterham, P., Daborn, P.J., 2012. A cytochrome p450 conserved in insects is involved in cuticle formation. PloS One 7, e36544.
Tilney, L.G., Connelly, P.S., Vranich, K.A., Shaw, M.K., Guild, G.M., 2000. Actin filaments and microtubules play different roles during bristle elongation in Drosophila. J. Cell Sci. 113 (Pt 7), 1255–1265.
Tilney, L.G., Tilney, M.S., Guild, G.M., 1995. F actin bundles in Drosophila bristles. I. Two filament cross-links are involved in bundling. J. Cell Biol. 130, 629–638.
Turner, C.M., Adler, P.N., 1998. Distinct roles for the actin and microtubule cytoskeletons in the morphogenesis of epidermal hairs during wing development in Drosophila. Mech. Dev. 70, 181–192.
Usui, T., Shima, Y., Shimada, Y., Hirano, S., Burgess, R.W., Schwarz, T.L., Takeichi, M., Uemura, T., 1999. Flamingo, a seven-pass transmembrane cadherin, regulates planar cell polarity under the control of Frizzled. Cell 98, 585–595.
Venema, D.R., Zeev-Ben-Mordehai, T., Auld, V.J., 2004. Transient apical polarization of Gliotactin and Coracle is required for parallel alignment of wing hairs in Drosophila. Dev. Biol. 275, 301–314.
Winter, C.G., Wang, B., Ballew, A., Royou, A., Karess, R., Axelrod, J.D., Luo, L., 2001. Drosophila Rho-associated kinase (Drok) links frizzled-mediated planar cell polarity signaling to the actin cytoskeleton. Cell 105, 81–91.
Wong, L.L., Adler, P.N., 1993. Tissue polarity genes of Drosophila regulate the subcellular location for prehair initiation in pupal wing cells. J. Cell Biol. 123, 209–221.
Wu, J., Mlodzik, M., 2009. A quest for the mechanism regulating global planar cell polarity of tissues. Trends Cell Biol. 19, 295–305.
Xu, J., Lan, L., Bogard, N., Mattione, C., Cohen, R.S., 2011. Rab11 is required for epithelial cell viability, terminal differentiation, and suppression of tumor-like growth in the Drosophila egg chamber. PLoS One 6, e20180.
Xu, T., Rubin, G.M., 1993. Analysis of genetic mosaics in developing and adult Drosophila tissues. Development 117, 1223–1237.
Zhao, H., Hakala, M., Lappalainen, P., 2010. ADF/cofilin binds phosphoinositides in a multivalent manner to act as a PIP(2)-density sensor. Biophys. J. 98, 2327–2336.